IOP PUBLISHING CLASSICAL AND QUANTUM GRAVITY

Class. Quantum Grav. **24** (2007) S501–S511 doi:10.1088/0264-9381/24/19/S13

# Searching for massive black hole binaries in the first Mock LISA Data Challenge

**Neil J Cornish**[1] **and Edward K Porter**[1,2]

[1] Department of Physics, Montana State University, Bozeman, 59717 MT, USA
[2] Max Planck Institut für Gravitationsphysik, Albert Einstein Institut, Am Mühlenberg 1, Golm, Germany

Received 30 January 2007, in final form 4 May 2007
Published 19 September 2007
Online at stacks.iop.org/CQG/24/S501

**Abstract**

The Mock LISA Data Challenge is a worldwide effort to solve the LISA data analysis problem. We present here our results for the massive black hole binary (BBH) section of round 1. Our results cover challenge 1.2.1, where the coalescence of the binary is seen, and challenge 1.2.2, where the coalescence occurs after the simulated observational period. The data stream is composed of Gaussian instrumental noise plus an unknown BBH waveform. Our search algorithm is based on a variant of the Markov chain Monte Carlo method that uses Metropolis–Hastings sampling and thermostated frequency annealing. We present results from the training data sets where we know the parameter values *a priori* and the blind data sets where we were informed of the parameter values after the challenge had finished. We demonstrate that our algorithm is able to rapidly locate the sources, accurately recover the source parameters and provide error estimates for the recovered parameters.

PACS numbers: 04.30.−w, 04.80.Nn

(Some figures in this article are in colour only in the electronic version)

## 1. Introduction

Massive black hole binaries (BBHs) are expected to be one of the strongest candidate sources for the Laser Interferometer Space Antenna (LISA), a joint ESA–NASA mission that will search for gravitational waves (GW) in the frequency bandwidth $10^{-5} \leqslant f/\mathrm{Hz} \leqslant 1$ [1]. The detection of BBHs by LISA is important for many reasons. First, it will allow us to carry out a test of general relativity in the highly nonlinear strong-field regime [2–4]. Second, it will allow us, in conjunction with other astronomical methods, to investigate such things as galaxy interactions and mergers out to very high redshift ($z \geqslant 10$). It will also allow us to test galaxy formation models such as hierarchical formation, where it is believed that modern-day galaxies were formed from the successive mergers of smaller 'seed' galaxies. Due to their

  

high masses, the inspiral phases for these systems occur at frequencies which are unavailable to the ground-based detectors due to their low-frequency cutoffs. Also, unlike galactic binaries and extreme mass ratio inspirals (EMRIs), the BBHs are very clean sources with detectable signal-to-noise ratios (SNR) of order ∼10–1000 s. This means that we will not have to deal with confusion noise between sources [5], something which is very important in the search for galactic binaries and to a lesser extent in the search for EMRIs.

Here we describe our analysis of the BBH component of the mock LISA data challenge [6]. This first round challenge is a simplified LISA problem where it is assumed that there is a single BBH buried in instrumental noise. Future rounds will consider the more realistic situation of multiple sources buried in instrumental noise plus a galactic foreground. Our search algorithm is a variant of the Markov chain Monte Carlo (MCMC) method which has been successfully implemented in [5, 8, 9] for searches involving single and multiple BBH sources immersed in both instrumental noise and galactic foreground of ∼30 million individually simulated galactic binaries. The algorithm uses a mixture of frequency annealing with thermostated heat, simulated annealing, plus a 5D exploration of the posterior distributions for the search parameters (we use a generalized $\mathcal{F}$-statistic to automatically search over the distance, inclination, polarization and initial phase). We refer the reader to [5] for a full description of the algorithm.

For the first challenge it was decided that the BBH would be modelled using a Schwarzschild restricted post-Newtonian waveform, where the amplitude is described by the dominant Newtonian harmonic, but the phase is evolved to a second post-Newtonian order. The waveform is described by the parameter set $\vec{x} = \{M_c, \mu, \theta, \phi, t_c, \iota, \psi, \Phi_0, D_L\}$, where the parameters in order are chirp mass, reduced mass, ecliptic latitude, ecliptic longitude, time of coalescence of the binary, inclination, GW polarization angle, initial orbital phase and luminosity distance. For each challenge, two data sets were issued. A training set where groups were informed of the answer *a priori* and a blind set where the groups were informed of the answer *a posteriori*. The training sets were issued to allow the different groups to test their algorithms.

In our earlier work we used the low-frequency approximation (LFA) [10] to model the instrument response, but to our surprise this proved to be insufficiently accurate for the MLDC data sets where the full detector response is used. Since the maximum frequencies of the injected signals were below 2 mHz, we had expected the LFA to be adequate, but when running on the training data sets we found systematic offsets in many of the parameters. The parameter recovery improved significantly when we upgraded our instrument response to the rigid adiabatic approximation (RAA) [11], which includes finite armlength effects. Our interpretation of this finding is that while the differences between the LFA and RAA are small at 2 mHz, the differences are amplified by the very large contribution to the signal-to-noise ratio that comes from the final cycles of the inspiral. Indeed, we suspect that the remaining small systematic offsets in the recovered masses can be traced to the approximate nature of the RAA.

We modified our barycentre waveforms and signal tapers to agree with those used to inject the simulated signals [12], but rather than searching over initial phase (the phase parameter used to generate the waveforms) we continued our earlier practice of searching over the phase at coalescence, as we have found this to give better acceptance rates in the search chains.

The organization of the rest of the paper is as follows. In section 2 we present a very short discussion of the search algorithm used. We define the Metropolis–Hastings sampling, the frequency annealing with thermostated heat and the simulated annealing scheme used. Section 3 contains a presentation of the results for both the training and blind data sets for the challenges.

## 2. The search algorithm

Our search algorithm, which is again explained in more detail in [5], is based on a Metropolis–Hastings sampling, which is the central engine of the standard Markov chain Monte Carlo method. Our method incorporates both simulated and frequency annealing schemes at various stages in the search. The algorithm uses a number of proposal distributions which we hope will mimic the posterior distribution to jump around the parameter space, as well as a maximization over the time to coalescence. To quickly summarize, starting with the signal $s(t)$ and some initial template $h(t, \vec{x})$ in the parameter space defined by the parameter set $\vec{x}$, the (un-normalized) posterior density $p(s|\vec{x})$ at $\vec{x}$ is computed. In this particular case the posterior density is defined by the likelihood

$$p(s|\vec{x}) = \mathcal{L}(\vec{x}) = C\, \mathrm{e}^{-\langle s-h(\vec{x}|s-h(\vec{x})\rangle}, \tag{1}$$

where $C$ is a normalization constant.

We then draw from a proposal distribution and propose a jump to another point in the parameter space defined by the set $\vec{y}$. The posterior and proposal densities at $\vec{x}$ and $\vec{y}$ are then compared by forming the Metropolis–Hastings ratio

$$H = \frac{\pi(\vec{y})\, p(s|\vec{y}) q(\vec{x}|\vec{y})}{\pi(\vec{x})\, p(s|\vec{x}) q(\vec{y}|\vec{x})}. \tag{2}$$

Here $\pi(\vec{x})$ are the priors of the parameters which we define to constrain the boundaries of the search, $p(s|\vec{x})$ is the likelihood and $q(\vec{x}|\vec{y})$ is the proposal distribution. This jump is then accepted with probability $\alpha = \min(1, H)$; otherwise the chain stays at the proposal point.

The likelihood was calculated using a generalized $\mathcal{F}$-statistic [13], which allows for an analytic extremization over the extrinsic parameters: luminosity distance, orbital inclination, polarization and orbital phase at coalescence. Consequently, the Markov chain portion of our search returns a marginalized posterior distribution. For future challenges we intend to follow the initial detection with a full parameter search so as to obtain the full posterior.

In the first section of the search we use a frequency annealing scheme to speed up the search. The search templates and the inner products used to compute the $\mathcal{F}$-statistic are terminated at a cutoff frequency $f_{\mathrm{cut}}$, which is initially set at $4 \times 10^{-5}$ Hz. The cutoff frequency is then increased as the chain progresses according to

$$f_{\mathrm{cut}} = \begin{cases} 10^{-B(1-\frac{i}{N_{fa}})} & f < f_{\mathrm{max}} \\ f_{\mathrm{max}} & f \geqslant f_{\mathrm{max}}, \end{cases} \tag{3}$$

where $i$ is the number of steps in the chain, $N_{fa}$ is the length of the frequency annealing chain, $B = \log\left(f_{\mathrm{max}} \big/ \left(f_{\mathrm{cut}}^{\mathrm{ini}}\right)\right)$ is a growth parameter, $f_{\mathrm{max}}$ is the maximum frequency the signals could reach given the priors on the masses etc and $f_{\mathrm{cut}}^{\mathrm{ini}}$ is the initial arbitrary cutoff frequency. As the cutoff frequency is incremented, more of the BBH signal is revealed and the SNR of the best-fit templates increases. Thus, frequency annealing acts in a similar way to traditional simulated annealing, but with the added benefit of saving in the cost of the template generation and $\mathcal{F}$-statistic computation. In testing we found that the search chains would sometimes lock onto secondary maxima during the frequency annealing phase, so we introduced a 'thermostating' procedure to control the effective SNR of the recovered signals. This was done by multiplying the noise spectral density in the noise-weighted inner products by a 'heat' factor $\beta$ which was adjusted based on the SNR of the current template,

$$\beta = \begin{cases} 1.0 & 0 \leqslant \mathrm{SNR} \leqslant 20 \\ \left(\dfrac{\mathrm{SNR}}{20}\right)^2 & \mathrm{SNR} > 20. \end{cases} \tag{4}$$

Once the frequency annealing stage was completed, the chain was cooled using the simulated annealing scheme,

$$\beta = \begin{cases} 10^{-\xi(1-\frac{j}{N_c})} & 0 \leqslant j \leqslant T_c \\ 1 & j > N_c, \end{cases} \tag{5}$$

with $\xi = \log_{10} \beta_{\max}$, where $\beta_{\max}$ is the heat factor at the end of the frequency annealing stage. The index $j$ counts from the end of the frequency annealing and the cool down lasts $N_c$ steps. A standard MCMC exploration of the marginalized posterior distribution function (PDF) commences once $\beta = 1$ and continues for $N_e$ steps. Finally, over the course of $N_f$ steps, we freeze the chain to a heat of $\beta = 0.01$ to aid in the extraction of maximum likelihood estimates (MLEs) for each of the parameters.

## 3. Conducting the challenge

The MLDC for binary black holes was broken into two parts. Challenge 1.2.1 had a source that coalesced inside the observation period, while challenge 1.2.2 had a source coalescing outside the observation period. The data sets provided consisted of $2^{21}$ data points sampled every 15 s giving approximately 1 year of data.

### *3.1. Challenge 1.2.1*

Priors on the source parameters were given for each challenge. For challenge 1.2.1, we were told that mass ranges were restricted such that $m_1 \in [1, 5] \times 10^6 M_\odot$ and $m_2 = m_1/x$, where $1 \leqslant x \leqslant 4$, and that the time to coalescence lay in the range $t_c \in [5, 7]$ months. We were also told that the system would have a signal to noise in the range $450 \leqslant \mathrm{SNR} \leqslant 500$ in one interferometer. No priors were given on the other source parameters. In addition to the blind data set, a training data set was made available with parameters drawn from the same set of priors.

For the 1.2.1 training data set we ran several 50 000 point chains. These chains were composed of a 10 000 point frequency annealing search, a 10 000 point simulated annealing phase cooldown, a 20 000 point MCMC chain to explore the PDFs and a final 10 000 point freezing of the chain to extract the MLEs. In figure 1 we plot three different search chains for eight of the nine waveform parameters in the 1.2.1 training set. We have omitted the search chain for the initial phase. We plot the extrinsic parameter chains even though their values were determined by analytical extremization at each point in the chain. While the angular variables employ a linear scale for the number of steps in the search, the other parameters are plotted against a logarithmic scaling to highlight the early convergence that occurs for the parameters such as the time to coalescence and the masses. The training data set provided for challenge 1.2.1 proved to be more challenging than similar test cases we generated for ourselves. In particular, the sky position of the source was not recovered to the accuracy predicted by a Fisher matrix estimate of the measurement errors. We attribute this to an unfortunate alignment of the source with respect to the LISA at the time of coalescence. At coalescence, the motion of the detector turns out to be perpendicular to line of sight to the source, so there is little or no Doppler shift of the gravitational waves right at the time when most of the SNR is accumulating. Thus, directional information gets less weighting than is typical, and the small differences between the RAA and the full response used to generate the

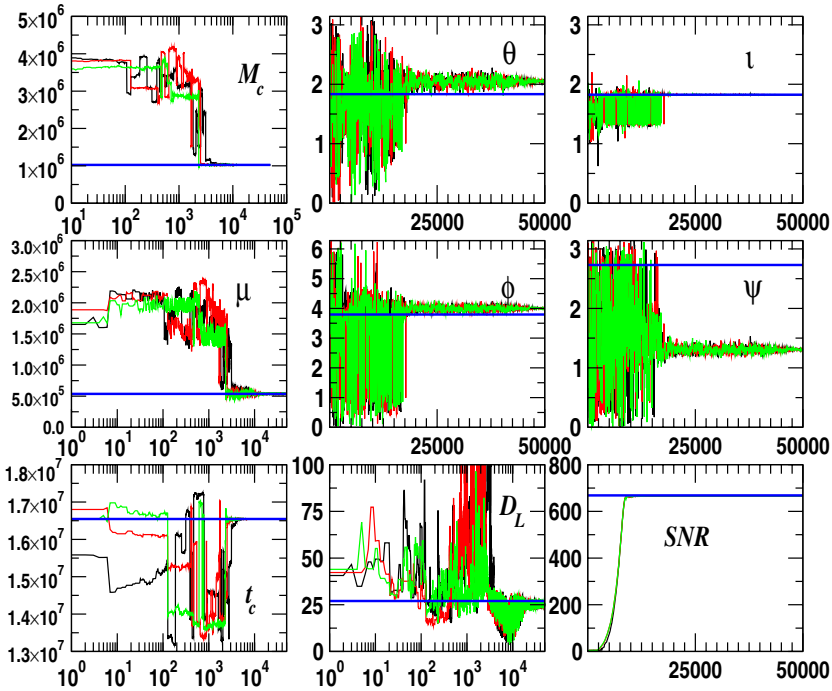


**Figure 1.** A plot of three search chains for eight of the nine parameters in the challenge 1.2.1 training set. The solid lines in each cell denote the true value. All angular variables are measured in radians, $M_c$ and $\mu$ have units of $M_\odot$, $t_c$ is given in seconds and $D_L$ is quoted in Gpc.

data sets are amplified. The only option then left for the chain is to compensate for the lack of sky information by varying the values of $(M_c, \mu, t_c)$ more than normal. The problem went away when we tested our search algorithm on the same source using data that were simulated with the RAA. In future challenges we plan to use a full detector response model to generate the search templates.

The sky location for the 1.2.1 blind data set proved to be easier to pin down and we were able to get away with shorter search chains of 25 000 points. These chains were composed of a 5000 point frequency annealing search, a 5000 point simulated annealing phase cooldown, a 10 000 point MCMC chain to explore the PDFs at unit heat and ending with a 5000 point freezing of the chain to extract the MLEs. We have plotted the search chains for the blind data set in figure 2, along with the values of the injected source parameters which were revealed after we had submitted our results. We see that the chains typically find the three most important parameters $(M_c, \mu, t_c)$ in around 1000 steps. Once again the sky positions took longer to converge, but in this instance the chains converged on the injected parameter values. The search also accurately recovered the extrinsic parameters, saved for the initial phase. The failure to recover the initial phase was due to a bug in our $\mathcal{F}$-statistic routine that we overlooked when working on the training data. We should also mention that while the recovered value for the polarization $\psi$ is off by $\pi$ from what was injected, the polarization angle is only defined up to multiples of $\pi$ so the solution is physically identical.

In figure 3 we have plotted the marginalized PDFs for the intrinsic parameters based on the merged MCMC chains from each different run. The solid line in each cell is the Fisher

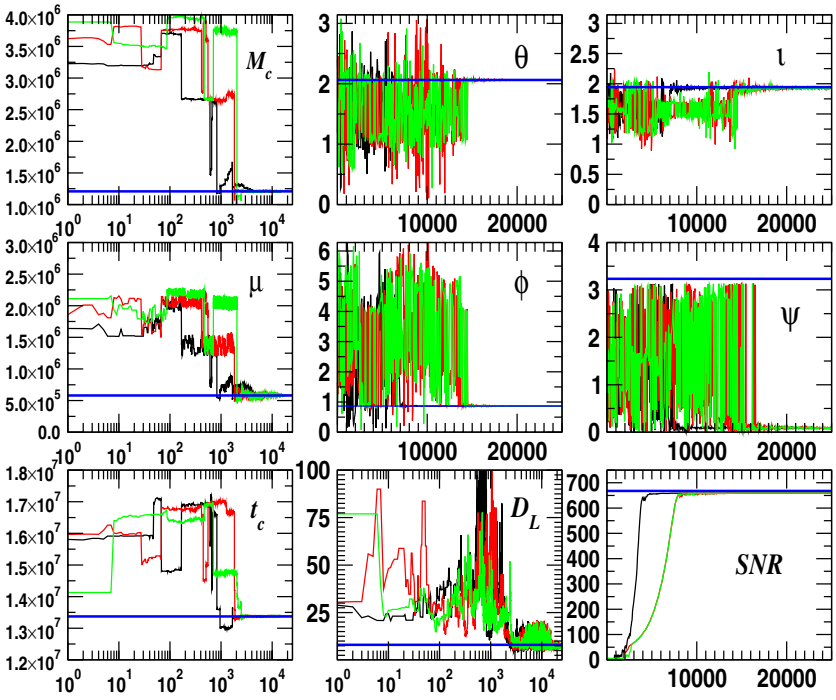


**Figure 2.** A plot of three search chains for eight of the nine parameters for the blind challenge 1.2.1 data set. The solid lines in each cell denote the true value. All angular variables are measured in radians, $M_c$ and $\mu$ have units of $M_\odot$, $t_c$ is given in seconds and $D_L$ is quoted in Gpc.

matrix prediction for the marginalized posteriors. While the chains were not long enough to fully characterize the posteriors, we see that the merged chains show good agreement with Fisher predictions for $(M_c, \theta, \phi)$. The Fisher predictions for $(\mu, t_c)$ do not agree very well with the MCMC results. At this time we do not have an explanation for the disagreement.

In table 1 we compare the values of the key file $\lambda^X$ against the MLEs $\lambda^{\rm MLE}$ for the training set (top) and the blind set (bottom). We also quote the $1\sigma$ error estimation from the Fisher matrix $\sigma^{\rm Fisher}_{\lambda^X}$ based on the key file values and the error in multiples of the $1\sigma$ error estimates from the Fisher matrix, i.e. $(\lambda^X - \lambda^{\rm MLE})/\sigma^{\rm Fisher}_{\lambda^X}$. While again we did not search for them, the MLEs obtained for $(\iota, \ln D_L, \psi)$ give errors of $(3.86 \times 10^{-3}, 6.62 \times 10^{-2}, 1.43)$ and $(1.7 \times 10^{-2}, 4.15 \times 10^{-2}, -2.7 \times 10^{-4})$ for the training and blind data sets respectively. The $\psi$ value is obtained from converting $\psi \to \psi + \pi$. For the blind data set, the source had a combined SNR of 664.78, while we recovered an SNR of 658.38. Again the mismatch is due, we feel, to a phasing issue in the code which has since been rectified. The new codes recover the initial phase almost perfectly. Each run took approximately 24 h on a single Mac G5 processor.

### *3.2. Challenge 1.2.2*

The priors for challenge 1.2.2 gave a time to coalescence of $400 \pm 40$ d and masses chosen such that $m_1 \in [1, 5] \times 10^6 M_\odot$ and again $m_2 = m_1/x$, where $1 \leqslant x \leqslant 4$. No priors were given on the other six parameters, save that the source would have an SNR in the range of

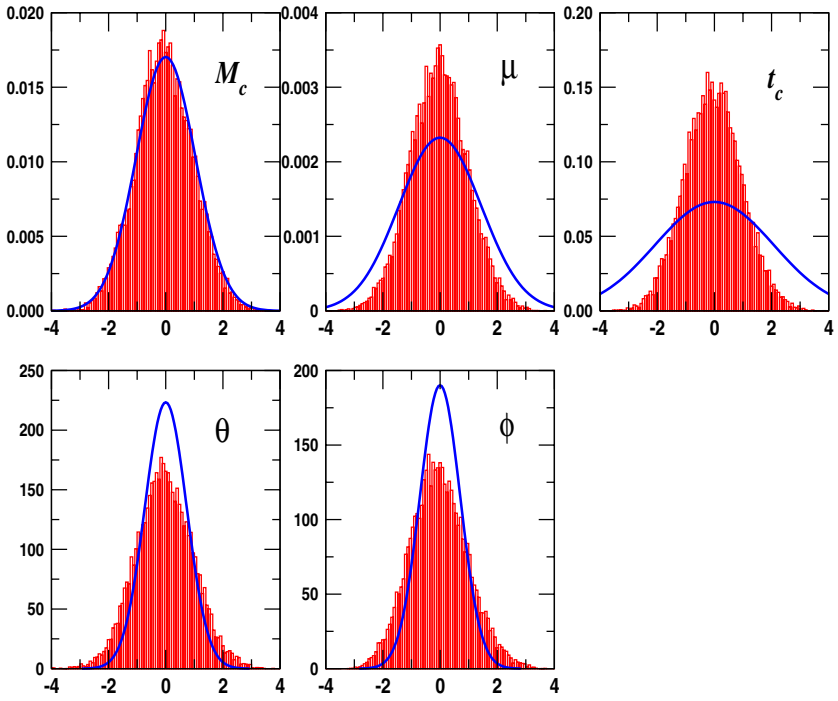


**Figure 3.** A comparison of the marginalized PDFs from the MCMC chains for the intrinsic parameters of 1.2.1 against the Fisher prediction (solid line) from the mean of the chain. The means of the chain have been subtracted and the values scaled by the square root of the variances of the chains.

**Table 1.** This table compares the injected parameter values, the MLE for each parameter, the $1\sigma$ error predicted by the Fisher matrix at the injected values, and the difference between the MLEs and the injected values in multiples of the Fisher $1\sigma$ error estimate for the challenge 1.2.1 training set (top) and blind set (bottom).

| | $\lambda^X$ | $\lambda^{\rm MLE}$ | $\sigma^{\rm Fisher}_{\lambda^X}$ | $\frac{\lambda^X-\lambda^{\rm MLE}}{\sigma^{\rm Fisher}_{\lambda^X}}$ |
|---|---|---|---|---|
| $M_c(M_\odot)$ | $1.023\,866\times10^6$ | $1.024\,227\times10^6$ | 45.06 | −8.01 |
| $\mu$ $(M_\odot)$ | $5.373\,042\times10^5$ | $5.389\,75\times10^5$ | 269.55 | −6.19 |
| $\theta$ (rad) | 1.8339 | 2.0488 | $6.673\times10^{-2}$ | −3.22 |
| $\phi$ (rad) | 3.7945 | 0.39981 | $4.414\times10^{-2}$ | −4.61 |
| $t_c$(s) | $1.654\,5493\times10^7$ | $1.654\,541\,8772\times10^7$ | 13.67 | 5.43 |
| $M_c(M_\odot)$ | $1.208\,59\times10^6$ | $1.2087\times10^6$ | 23.78 | −5.004 |
| $\mu$ $(M_\odot)$ | $5.811\,96\times10^5$ | $5.818\times10^5$ | 173.35 | −3.5 |
| $\theta$ (rad) | 2.0631 | 2.0619 | $1.81\times10^{-3}$ | 0.63 |
| $\phi$ (rad) | 0.8658 | 0.8645 | $2.12\times10^{-3}$ | 0.63 |
| $t_c$(s) | $1.337\,4027\times10^7$ | $1.337\,4031\times10^7$ | 5.53 | −0.62 |

$20 \leqslant \mathrm{SNR} \leqslant 100$ in one interferometer. For both the training and blind sets, we used 25 000 point search chains. These chains were composed of a 5000 point frequency annealing search, a 5000 point simulated annealing phase cooldown, a 10 000 point MCMC chain to explore the PDFs at unit heat and ending with a 5000 point freezing of the chain to extract the MLEs.

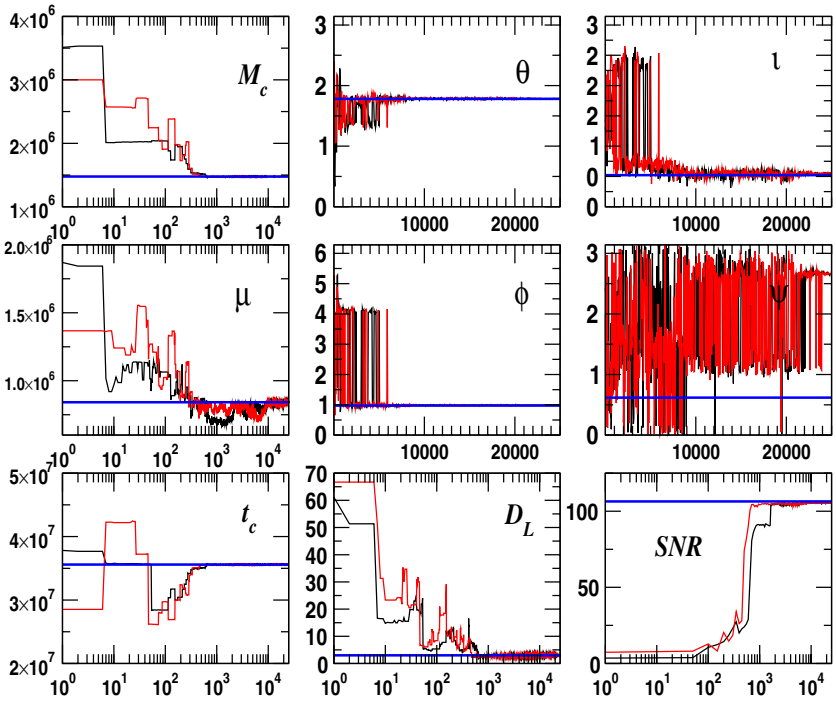


**Figure 4.** A plot of three search chains for eight of the nine parameters of the challenge 1.2.2 training data set. The solid lines in each cell denote the true value. All angular variables are measured in radians, $M_c$ and $\mu$ have units of $M_\odot$, $t_c$ is given in seconds and $D_L$ is quoted in Gpc.

In figure 4 we plot three search chains for the training data set. The chirp mass and time to coalescence are recovered in under 1000 steps. For this particular source, the chains also rapidly converge on the correct sky position. Again, while not explicitly searched for, the search correctly recovered the inclination of the orbit and luminosity distance. However, the recovered polarization angle is not very good. We should note here that we have mapped the key file value back into a $0$–$\pi$ range.

In figure 5 we plot three search chains for the blind data set. All five intrinsic parameters lock-in after a few thousand steps. Except for the luminosity distance, the extrinsic parameters are far from the true values. We attribute this to the fact that the phase at coalescence is essentially undetermined for systems where we do not see coalescence. In figure 6 we plot the marginalized PDFs for the intrinsic parameters based on the merged MCMC chains from multiple runs. The solid line in each cell is the prediction of the Fisher matrix at the mean of the chain. There is a discrepancy between the Fisher prediction and the posteriors from the chains. A visual inspection of the chains indicates a large autocorrelation that extends over thousands of points. This slow mixing of the chains implies that we would need to run much longer MCMC segments in order to get meaningful posterior distributions to compare to the Fisher predictions.

In table 2 we compare the values of the injected parameters against the MLEs. We again quote the $1\sigma$ error estimation from the Fisher matrix and the error in multiples of the Fisher matrix based on the MLEs. Also, based on the $\mathcal{F}$-statistic search for the intrinsic parameters, the MLEs obtained for $(\iota, \ln D_L, \psi)$ give errors of $(-0.0313, 0.0124, 1.09)$ and

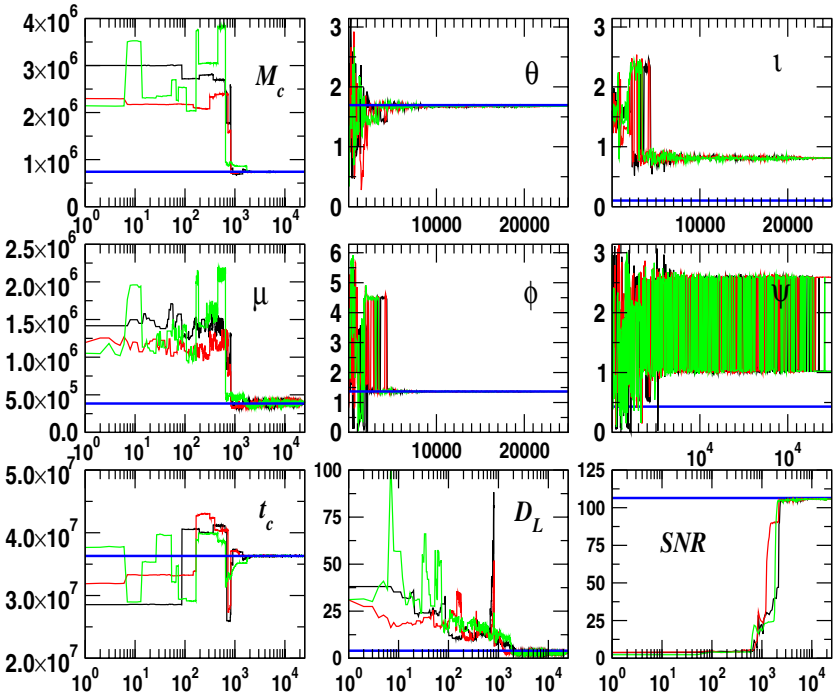


**Figure 5.** A plot of three search chains for eight of the nine blind parameters in challenge 1.2.2. The solid lines in each cell denote the true value. All angular variables are measured in radians, $M_c$ and $\mu$ have units of $M_\odot$, $t_c$ is given in seconds and $D_L$ is quoted in Gpc.

**Table 2.** This table shows the injected parameter values, the MLE for each parameter, the $1\sigma$ error predicted by the Fisher matrix at the injected values and the difference between the MLEs and the injected values in multiples of the Fisher $1\sigma$ error estimate for the challenge 1.2.2 training set (top) and blind data set (bottom).

| | $\lambda^X$ | $\lambda^{\rm MLE}$ | $\sigma^{\rm Fisher}_{\lambda^X}$ | $\frac{\lambda^X-\lambda^{\rm MLE}}{\sigma^{\rm Fisher}_{\lambda^X}}$ |
|---|---|---|---|---|
| $M_c(M_\odot)$ | $1.476\,37\times10^6$ | $1.4765\times10^6$ | 209.5 | −0.66 |
| $\mu$ $(M_\odot)$ | $8.4183\times10^5$ | $8.4748\times10^5$ | 8466.8 | −0.67 |
| $\theta$ (rad) | 1.7802 | 1.7862 | $4.09\times10^{-3}$ | 1.47 |
| $\phi$ (rad) | 0.9737 | 0.9904 | $4.22\times10^{-3}$ | −3.95 |
| $t_c$ (s) | $3.559\,836\times10^7$ | $3.559\,978\times10^7$ | 2361.8 | −0.6 |
| $M_c(M_\odot)$ | $7.4146\times10^5$ | $7.4169\times10^5$ | 97.78 | −2.35 |
| $\mu$ $(M_\odot)$ | $3.848\times10^5$ | $3.989\times10^5$ | 5273.4 | −2.66 |
| $\theta$ (rad) | 1.6947 | 1.6758 | $5.1\times10^{-3}$ | 3.73 |
| $\phi$ (rad) | 1.3674 | 1.362 | $5.27\times10^{-3}$ | 1.03 |
| $t_c$ (s) | $3.630\,76\times10^7$ | $3.631\,42\times10^7$ | 2827.7 | −2.33 |

$(-0.71, 0.273, -2.16)$ for the training and blind data sets respectively. The source had a combined SNR of 106.54, while we recovered an SNR of 105.72. Each run took approximately 6 h on a single 2 GHz Mac G5 processor.

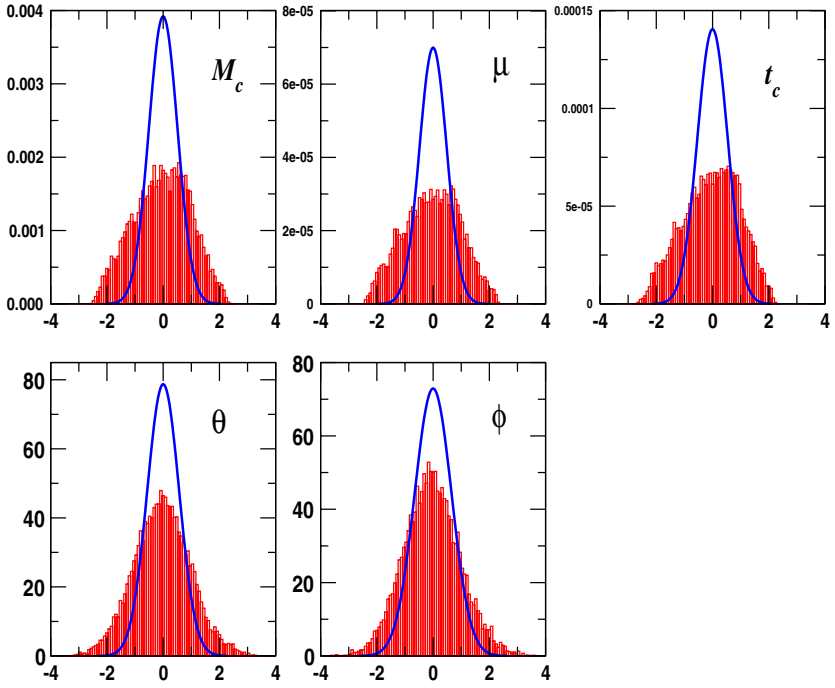


**Figure 6.** A comparison of the marginalized PDFs from the MCMC chains for the intrinsic parameters of 1.2.2 against the Fisher prediction (solid line) from the mean of the chain. The means of the chain have been subtracted and the values scaled by the square root of the variances of the chains.

## 4. Conclusion

The mock LISA data analysis challenge data sets for binary black hole inspirals proved to be a valuable testing ground for our Metropolis–Hastings search algorithm. Overall the algorithm performed very well, recovering the injected parameters to an accuracy largely consistent with the theoretical error margins. There were also some surprises, such as needing to go over to a more accurate treatment of the instrument response in our template generation and a problem with our conventions when extracting the initial orbital phase. We have displayed in [5] that the MCMC method has no problem in searching for and identifying multiple BBH sources. In the case of multiple sources, our chains always jump between sources initially, but eventually always lock onto the highest SNR source first. By using an iterative search-and-extract routine, we have found we can extract the bright sources first and work our way down to the dimmer sources. Work is now underway on the much more complicated multi-source challenge 2 data sets, and early results from runs on the training data look very promising.

## Acknowledgments

This work was supported at MSU by NASA grant NNG05GI69G.

## References

[1] Bender P *et al* 1998 *LISA Pre-Phase: A report* http://lisa.gsfc.nasa.gov/Documentation/ppa2.08.pdf
[2] Ryan F D 1997 *Phys. Rev.* D **56** 1845

[3] Collins N A and Hughes S A 2004 *Phys. Rev.* D **69** 124022
[4] Berti E, Cardoso V and Will C M 2006 *Phys. Rev.* D **73** 064030
[5] Cornish N J and Porter E K 2006 *Preprint* gr-qc/0612091
[6] Arnaud K A *et al* 2006 *Preprint* gr-qc/0609105
[7] http://astrogravs.nasa.gov
[8] Cornish N J and Porter E K 2006 *Class. Quantum Grav.* **23** S761
[9] Cornish N J and Porter E K 2007 *Phys. Rev.* D **75** 021301
[10] Cutler C 1998 *Phys. Rev.* D **57** 7089
[11] Rubbo L J, Cornish N J and Poujade O 2004 *Phys. Rev.* D **69** 082003
[12] MLDC Challenge 1 Omnibus Document http://svn.sourceforge.net/viewvc/lisatools/Docs/challenge1.pdf
[13] Jaranowski P, Królak A and Schutz B F 1998 *Phys. Rev.* D **58** 063001